The Astrophysical Journal Supplement Series, 173:85–103, 2007 November

FAINT H I 21 cm EMISSION LINE WINGS AT FORBIDDEN VELOCITIES

Ji-hyun Kang and Bon-Chul Koo
Astronomy Program, Department of Physics and Astronomy, Seoul National University, Seoul 151-747, Korea;
kjh@astro.snu.ac.kr, koo@astrohi.snu.ac.kr
Received 2007 January 24; accepted 2007 May 7

ABSTRACT

We present the results of a search for faint H I 21 cm emission line wings at velocities forbidden by Galactic rotation in the Galactic plane using the Leiden/Dwingeloo H I Survey data and the H I Southern Galactic Plane Survey data. These "forbidden-velocity wings" (FVWs) appear as protruding excessive emission in comparison with their surroundings in limited ($\lesssim 2°$) spatial regions over velocity extents of more than $\sim$20 km s^{-1} in large-scale (ℓ, v) diagrams. Their high velocities imply that there should be some dynamical phenomena associated. We have identified 87 FVWs. We present their catalog and discuss their distribution and statistical properties. We found that 85% of FVWs are not coincident with known supernova remnants (SNRs), galaxies, or high-velocity clouds. Their natures are currently unknown. We suspect that many of them are fast-moving H I shells and filaments associated with the oldest SNRs that are essentially invisible except via their H I line emission. We discuss other possible origins.

Subject headings: ISM: general — ISM: kinematics and dynamics — ISM: structure — radio lines: ISM — supernova remnants

Online material: machine-readable table

1. INTRODUCTION

Large-scale (ℓ, v) diagrams of H I 21 cm line emission in the Galactic plane usually show faint high-velocity bumps protruding from their surroundings. These faint "wing"-like features are extended to the velocities well beyond the maximum or minimum velocities permitted by the Galactic rotation. Some of those "forbidden-velocity wings" (FVWs) are shown in Figure 1, which is a (ℓ, v) diagram of the Galactic H I emission in the first and the second quadrants at $b = -0.5°$. FVWs are the ones that are small and smoothly extend from the main Galactic H I, which distinguishes them from high-velocity clouds (HVCs) that have discrete peaks isolated from the Galactic H I. FVWs are probably the sites where kinetic energies are expelled into the interstellar medium (ISM) by some violent events.

Our interest about FVWs was first motivated by the statistics of SNRs, namely that the number of known SNRs is much less than expected (Koo & Kang 2004, hereafter KK04). The number of presently known Galactic SNRs, most of which have been identified in the radio continuum, is 265 according to Green's catalog (Green 2006),[1] which provides a most complete and up-to-date list of identified Galactic SNRs. This is much lower than the number (20,000–30,000) expected from the SN rate and the lifetimes of SNRs. Therefore, most SNRs are "missing," and it must be mainly old SNRs that are missing considering their large population. This is not surprising because old SNRs are faint in the radio continuum, and it is difficult to identify faint radio sources because of the confusion due to the Galactic background emission and also because of observational limitations (e.g., Brogan et al. 2006). KK04 paid attention to the fact that an old SNR consists of quickly expanding H I shell and that the shell might last after the remnant becomes too faint to be visible in the radio continuum. If its expansion velocity is greater than the minimum or maximum velocities permitted by the Galactic rotation, then the SNR shell or part of it (maybe the caps) could be detected as high-velocity gas, e.g., FVWs, in Figure 1. They proposed that the FVWs could be possible candidates for the missing old SNRs. Indeed, Koo et al. (2006) have carried out high-resolution H I line observations toward FVW 190.2+1.1, one of the FVWs in this paper, and detected a rapidly expanding ($\sim$80 km s^{-1}) H I shell. The parameters of this shell seem only consistent with those of the remnant of a SN explosion. This shell is not seen in any other wave band, suggesting that it represents the oldest type of SNR, which is essentially invisible except via its H I line emission.

Although an SNR is a strong candidate of FVWs, the high velocities of FVWs could be also produced by stars expelling their mass into the ISM, e.g., stellar winds from massive stars, and outflows from young stellar objects or asymptotic giant branch (AGB) stars. High- or intermediate-velocity clouds (HVCs, IVCs) that happen to be close to the maximum/minimum velocity of the H I gas along the line of sight would appear as FVWs, too. In order to understand the nature of FVWs and their relation to old SNRs, therefore, a systematic study of FVWs is required.

We have searched FVWs in the Galactic plane ($|b| \leq 13°$) using Leiden/Dwingeloo H I Survey (LDS) data and H I Southern Galactic Plane Survey (SGPS) data, and we have studied their statistical characteristics. Some of our preliminary results were published by Kang et al. (2004). In § 2, we explain the H I surveys used for the search and the identification procedure. The catalog of FVWs is presented in § 3, where we show their statistical properties and the result of comparison with other objects, too. The possibility of FVWs being SNRs, and some other possible origins, will be discussed in § 4. We finally summarize our results in § 5.

2. OBSERVATIONAL DATA AND IDENTIFICATION

2.1. *Data*

We used two sets of Galactic H I survey data; the Leiden/Dwingeloo H I survey (LDS; Hartmann & Burton 1997) and the Parkes survey, which is a part of the H I Southern Galactic Plane Survey (SGPS; McClure-Griffiths 2001).

The LDS was carried out with the 25 m Dwingeloo telescope (FWHM = 36′) on a half-degree grid using frequency-switching mode. The survey covered the sky north of declination $-30°$

[1] Available at http://www.mrao.cam.ac.uk/surveys/snrs/.

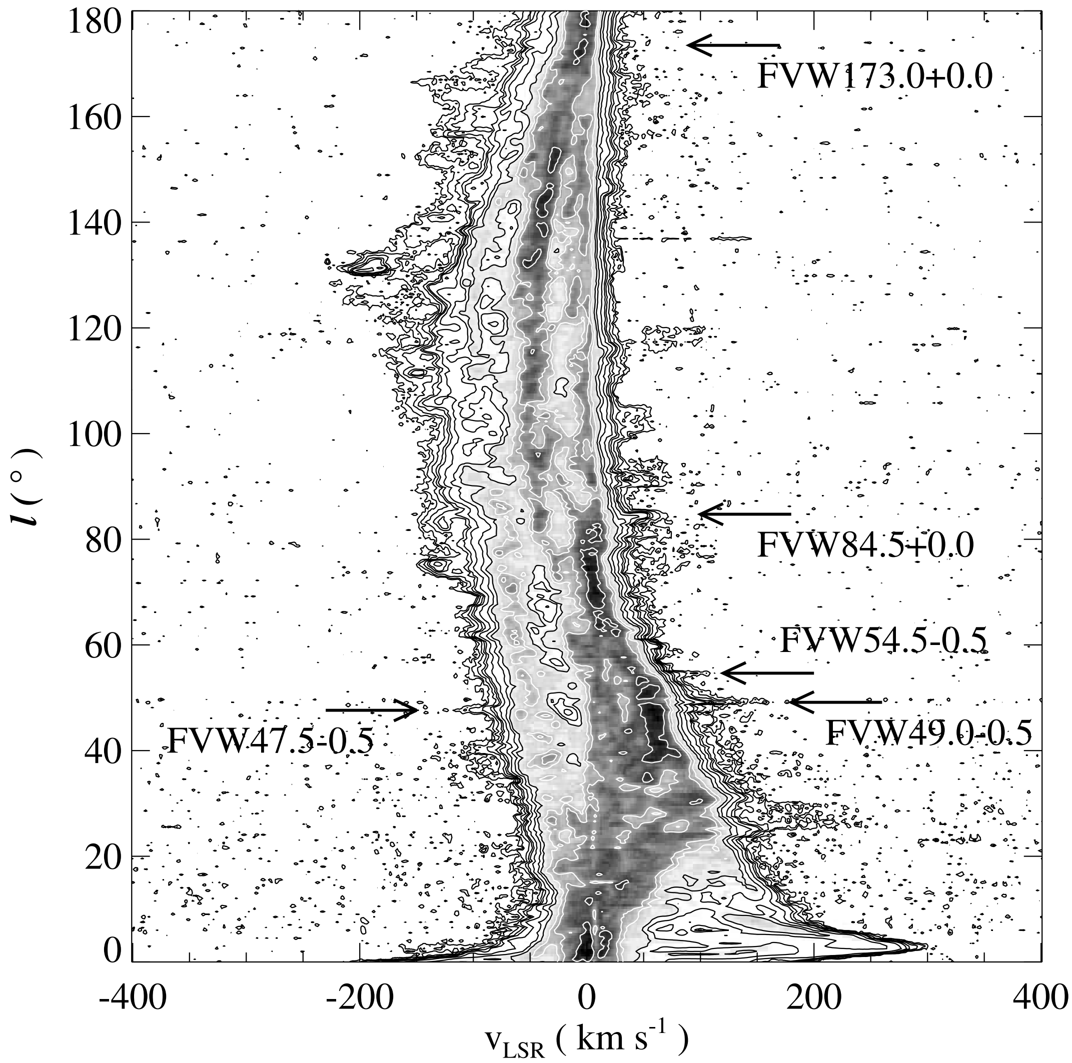

FIG. 1.—Large-scale (ℓ, v) diagram of the first and second quadrants at $b = -0.5°$. The LDS data are used. Contours are 0.1, 0.2, 0.4, 0.7, 1, 2, 5, 10, 30, 50, and 100 K in brightness temperature.

completely on this grid. Its effective velocity coverage spans local standard of rest (LSR) velocities from -450 to $+400$ km s^{-1}, resolved into spectral channels of 1.03 km s^{-1} width. Stray radiation correction is applied to LSD data. The nominal brightness-temperature sensitivity of the LDS is 0.07 K. The velocity resolution is not critical for the identification of FVWs because FVWs are extended over a rather wide velocity range. We smoothed each spectrum to a resolution of 3.09 km s^{-1}, so that the rms noise of the final cubes used for the identification becomes $\sim$0.05 K.

The Parkes survey is a part of SGPS, a survey of the H I spectral line and 21 cm continuum emission in the fourth quadrant of the Galactic plane. The Parkes survey covers $l = 253°$–$358°$ and $|b| \lesssim 10°$. The Parkes data were obtained with the inner seven beams of the Parkes multibeam system, a 13 beam 21 cm receiver package at prime focus on the Parkes 64 m radio telescope (FWHM $= 16'$), by the process of "on-the-fly" mapping. The final calibrated Parkes data consist of 10 cubes with a cell size of $4'$, and a velocity resolution of 0.82 km s^{-1} covering from -250 to $+200$ km s^{-1}. The rms noise of the survey in brightness temperature varies from 0.13 to 0.27 K depending on the cube. The main survey area ($|b| \le 1.5°$) was reobserved to put limits on the amount of stray radiation, so that the rms noise is significantly better in this area (0.09–0.14 K). For the coherence of this study, we convolved the Parkes data using a Gaussian beam to have the same angular resolution as the LDS and then regridded the data with a grid interval of 0.5°. The velocity channels are not smoothed (but just

TABLE 1

HIGHLY COMPLICATED AREAS IN (ℓ, v) DIAGRAMS

(ℓ_{min}, ℓ_{max})	(b_{min}, b_{max})	v_{LSR} (+ or −)	Note
(0°, 50°)	(−13°, −4°)	+	
(10°, 30°)	(+5°, +10°)	+	
(10°, 30°)	(+7°, +13°)	−	
(90°, 150°)	(−11°, −7°)	−	HVC complex G
(110°, 160°)	(−2°, +7°)	−	HVC complex H
(160°, 180°)	(−2°, +4°)	−	Anticenter shell
(160°, 200°)	(+4°, +13°)	−	Anticenter shell
(180°, 205°)	(−4.5°, +0°)	−	Anticenter shell
(260°, 330°)	(+5°, +10°)	+	
(330°, 360°)	(+6°, +10°)	+, −	
(330°, 360°)	(−10°, −4°)	+, −	

TABLE 2
CATALOG OF FORBIDDEN-VELOCITY WINGS

Name (FVW$\ell \pm b$)	$v_{\min}$, $v_{\max}$ (km s^{-1})	$\int \Delta \bar{T}_b \, dv$ (K km s^{-1})	Rank	Associated Object
FVW 6.5−2.5	−135, −108	3.3 ± 5.3	2	
FVW 10.0+7.5	−81, −39	28.6 ± 4.6	1	
FVW 15.5−10.5	−48, −17	14.9 ± 1.6	2	
FVW 18.0−6.5	−53, −23	16.3 ± 2.4	2	
FVW 20.0−5.5	−45, −24	3.7 ± 3.1	2	
FVW 27.5+6.5	−101, −75	10.0 ± 2.5	2	
FVW 34.0−1.5	117, 138	19.6 ± 8.4	1	
FVW 39.0+4.0	89, 131	35.2 ± 8.2	2	
FVW 40.0+0.5	−113, −80	21.9 ± 2.3	3	
FVW 44.5−2.0	79, 119	53.8 ± 14.2	1	
FVW 47.5−0.5	−111, −88	6.5 ± 0.8	3	
FVW 49.0−0.5	91, 138	34.9 ± 4.6	3	SNR, W51
FVW 51.5+3.5	71, 86	24.3 ± 9.7	1	
FVW 54.5−0.5	85, 105	2.8 ± 0.7	2	SNR, HC 40
FVW 69.0+2.5	35, 89	26.6 ± 5.6	3	SNR, CTB 80
FVW 71.0−4.0	−129, −103	57.4 ± 5.1	2	
FVW 75.5+0.5	30, 60	29.9 ± 3.0	1	
FVW 78.0+2.0	43, 57	13.0 ± 3.5	1	SNR, DR 4
FVW 79.0+1.0	35, 57	22.4 ± 5.6	1	
FVW 81.5+1.5	33, 53	41.0 ± 5.2	1	
FVW 83.5+4.0	30, 52	29.0 ± 5.7	1	
FVW 84.5+0.0	34, 55	45.9 ± 5.7	1	
FVW 86.0−9.5	20, 57	54.0 ± 7.7	2	
FVW 87.5−11.0	21, 42	12.0 ± 4.4	1	
FVW 88.5+5.0	30, 88	24.6 ± 5.2	3	SNR, HB 21
FVW 94.5+8.0	31, 114	18.5 ± 2.2	3	Galaxy, Cepheus 1
FVW 95.5+11.5	25, 180	45.3 ± 2.4	3	Galaxy, NGC 6946
FVW 95.5+7.0	26, 65	7.3 ± 2.4	3	
FVW 96.0+4.0	18, 38	14.3 ± 2.5	2	
FVW 96.5−6.0	28, 48	7.5 ± 1.3	1	
FVW 97.5−3.0	28, 52	5.5 ± 1.3	1	
FVW 99.5−7.5	11, 48	60.5 ± 12.2	2	
FVW 101.0−9.5	20, 57	28.9 ± 4.8	3	
FVW 104.5+2.0	20, 52	7.4 ± 1.4	3	
FVW 107.0+8.0	17, 58	15.2 ± 3.0	3	
FVW 108.0+7.0	27, 53	5.4 ± 2.0	3	
FVW 108.0+10.0	29, 51	3.2 ± 0.8	3	
FVW 109.5+2.5	8, 44	264.8 ± 40.3	3	
FVW 112.0−6.0	18, 36	11.7 ± 1.6	1	
FVW 112.0−2.0	39, 65	4.7 ± 0.8	1	SNR (?), Cassiopeia A
FVW 116.5+12.0	−196, −147	14.0 ± 1.8	3	
FVW 126.0−1.0	24, 55	5.1 ± 0.9	3	
FVW 128.0−10.5	9, 58	50.3 ± 5.8	2	
FVW 133.5+2.5	26, 47	1.5 ± 0.6	2	
FVW 138.0+10.5	16, 129	170.2 ± 12.0	3	Galaxy, UGC 2847
FVW 139.5+10.5	26, 155	32.7 ± 52.5	3	Galaxy, UGCA 86
FVW 166.5+0.5	29, 59	4.7 ± 1.0	2	
FVW 172.5+6.0	28, 86	11.2 ± 1.1	3	
FVW 173.0+0.0	22, 40	5.5 ± 1.8	2	
FVW 173.0+3.0	11, 40	57.0 ± 23.7	3	
FVW 190.2+1.1	44, 81	8.4 ± 1.6	3	
FVW 191.0−2.0	54, 82	5.7 ± 1.4	3	
FVW 196.5+1.5	−130, −58	74.8 ± 11.1	1	HVC
FVW 197.0+7.0	52, 78	4.4 ± 2.1	2	
FVW 201.0+9.5	64, 90	9.2 ± 0.8	3	

TABLE 2—*Continued*

Name (FVW$\ell \pm b$)	$v_{\rm min}$, $v_{\rm max}$ (km s^{-1})	$\int \Delta \bar{T}_b \, dv$ (K km s^{-1})	Rank	Associated Object
FVW 201.5−7.5	−56, −20	11.8 ± 4.2	1	
FVW 201.5−5.0	−60, −17	17.6 ± 3.9	1	
FVW 203.0+6.5	85, 132	22.4 ± 1.3	3	HVC
FVW 203.5+4.5	80, 106	5.5 ± 2.3	3	
FVW 211.5+9.0	66, 98	10.7 ± 3.8	1	
FVW 212.5+5.5	78, 115	9.8 ± 2.2	3	
FVW 212.5+3.5	67, 127	45.1 ± 13.5	2	
FVW 215.0+7.0	84, 115	11.1 ± 1.7	3	HVC
FVW 215.5+7.5	−43, −20	5.8 ± 0.8	3	
FVW 225.5+6.0	103, 128	7.2 ± 2.1	1	
FVW 233.5+5.0	114, 148	8.9 ± 1.6	1	
FVW 235.5−1.0	134, 155	4.0 ± 1.2	1	
FVW 238.5+0.5	141, 167	5.2 ± 0.9	3	
FVW 240.0+4.0	127, 153	7.6 ± 2.2	1	
FVW 242.5+2.0	141, 161	6.7 ± 1.7	1	
FVW 243.0−2.0	135, 167	19.0 ± 3.5	3	
FVW 251.0+12.0	−36, −13	27.9 ± 4.2	3	
FVW 252.5+10.5	−50, −30	6.6 ± 0.7	2	
FVW 260.9−1.9	159, 184	16.8 ± 5.9	2	
FVW 261.6+2.3	158, 178	13.9 ± 5.9	2	
FVW 283.4+3.0	−57, −42	13.0 ± 5.0	2	
FVW 291.0+2.9	−72, −55	17.9 ± 9.8	2	
FVW 293.0+7.9	−74, −53	20.5 ± 7.8	1	
FVW 298.3−3.7	135, 167	19.2 ± 8.4	1	
FVW 304.5−5.7	−91, −66	40.7 ± 13.4	2	
FVW 311.9−1.1	−109, −92	8.9 ± 4.1	2	
FVW 312.3+3.6	−99, −80	42.3 ± 36.1	2	
FVW 313.4+0.6	−117, −100	12.2 ± 4.8	2	
FVW 315.2+2.7	−107, −87	20.9 ± 8.9	1	
FVW 319.8+0.3	−123, −98	22.9 ± 8.1	3	
FVW 324.5+4.2	−132, −112	7.0 ± 4.8	2	
FVW 342.5+1.7	96, 110	3.9 ± 1.9	3	

NOTE.—Table 2 is also available in machine-readable form in the electronic edition of the *Astrophysical Journal Supplement*.

regridded to a grid of 1.03 km s^{-1} interval) because the resulting data cubes have rms noise (0.02–0.04 K) already lower than that of the LDS data cubes.

2.2. *Identification*

We have identified FVWs by drawing large-scale (ℓ, v) diagrams of each quadrant every 0.5° in Galactic latitude for Galactic latitudes of $|b| \le 13°$. All identification was carried out with the naked eye. We first selected areas protruding from the Galactic background H I emission at contours between 0.1 and about 1.0 K. Among them, we chose the ones with velocity extents greater than ~20 km s^{-1} compared to the neighborhood area. Then we looked into the channel images to make sure that their high-velocity features are clearly visible. We limited our selection only for those that are confined in small regions ($\lesssim 2°$). The $\lesssim 2°$ criterion is not based on an astrophysical consideration but is rather empirical. However, this should be a reasonable choice for identifying missing SNRs because most of them might reside in the inner Galaxy and smaller than ~2° (KK04).

In Figure 1, for example, the features near $\ell = 47°$, 49°, 54°, 84°, and 173° are selected. However, the ones confined in somewhat broad longitude regions (~5°) near $\ell = 27°$, 40°, and 100° are not selected. Those features do not seem to be real but rather caused by data reduction processes. In LDS data, the spectra in a 5° × 5° box are reduced at same time and these excess emissions are confined in 5° × 5° square areas almost exactly.

FVWs could not be identified in the areas where groups of HVCs, IVCs, or supershells make the velocity boundary complicated or where the velocity boundary is unclear or clumpy. For example, anticenter shell and HVC complexes H and G highly contaminate the negative velocity boundaries near $120° \lesssim \ell \lesssim 200°$, and some velocity boundaries at high latitudes in the inner Galaxy are clumpy due to many HVCs. Table 1 summarizes those areas. We note that there are gaps at $242° \lesssim \ell \lesssim 253°$, at $0° \lesssim \ell \lesssim 5°$, and at $350° \lesssim \ell \lesssim 360°$ between the two surveys. (The exact longitude interval depends on latitude.)

3. RESULTS

3.1. *The Catalog*

A total of 87 FVWs have been identified; 73 in the northern sky and 14 in the southern sky. The parameters of the FVWs are summarized in Table 2. The entries of the catalog are as follows:

(1) name of FVWs based on the Galactic coordinates (the central coordinates are determined in the images integrated over the given velocity extent; (2) velocity ranges where excess H I emission is seen; (3) integrated intensity of H I 21 cm line emission over the given velocity extent at the center of FVWs; (4) rank indicating definiteness of protruding feature [higher rank means it is more apparent in (ℓ, v) or (b, v) diagrams (see next paragraph)]; (5) associated celestial objects (see § 3.3).

We assign rank 3 to FVWs that are well-defined in both in the (ℓ, v) and (b, v) diagrams. The prototypical ones are FVW 49.0−0.5, FVW 94.5+8.0, FVW 203.0+6.5, etc. They are usually located in areas with flat and clear velocity boundaries. Rank 1 FVWs are those with relatively unclear high-velocity features in both the (ℓ, v) and (b, v) diagrams. The prototypical ones are FVW 10.0+7.5, FVW 51.5+3.5, FVW 201.5−7.5, etc. They are located in areas of complicated velocity boundaries but still show stronger emission than their surroundings over the velocity intervals in Table 2. We assign rank 2 to the rest, i.e., the ones that are relatively well-defined in the (ℓ, v) diagram but not in the (b, v) diagram, or vice versa. The prototypical ones are FVW 6.5−2.5, FVW 197.0+7.0, and FVW 311.9−1.1. Rank 3 includes 33 FVWs, and both rank 2 and rank 1 have 27 FVWs. We note that, for some FVWs, e.g., FVW 99.5−7.5, FVW 104.5+2.0, or FVW 196.5+1.5, the classification is ambiguous so that the ranks may be considered as a general guide of protrusion level. The integrated images and position-velocity diagrams of 87 FVWs are presented in Figure 2. Since identifying FVWs by eye is a subjective process, we note that the FVW catalog may be incomplete and needs a careful consideration for statistical interpretation (see next section).

3.2. *Statistical Properties*

Figure 3 presents the distribution of the FVWs in the (ℓ, b) plane with information about their LSR velocities and integrated intensities. FVWs are marked by different symbols depending on their associations with other known objects (see § 3.3). The center of each symbol indicates its Galactic coordinates, and the area presents its integrated intensity. The color indicates the mean velocity with the scales shown by the color bar on the top. The hatched areas represent the highly complicated areas in Table 1. The areas filled with solid black show gaps between data, and the dotted line shows the boundary of the search in latitude.

FVWs are scattered on the (ℓ, b) plane. They are neither clustered in the inner Galaxy nor strongly concentrated toward the Galactic plane. This is more clearly seen in the left and right panels of Figure 4, which show the distribution of FVWs in Galactic longitude and latitude, respectively. Along the Galactic longitude, there are relatively large number of FVWs between $\ell \approx 80°$ and 120° and perhaps at $\ell \approx 200°$, while the number is relatively small between $\ell \approx 140°$ and 180° and between $\ell \approx 330°$ and 10°. The distribution of FVWs in Galactic latitude is broad and slightly skewed to high positive latitudes. A Gaussian fitting yields $b = 2.3°$ as the center and 13.2° as the full width at half-maximum (FWHM) of the distribution. The FWHM in the inner Galaxy is smaller than that in the outer Galaxy, i.e., $\sim$8° and 17°, respectively.

A noticeable feature in Figure 3 is the change of the velocity of FVWs with Galactic longitude (see also Fig. 4, *left*). Between $\ell \sim 50°$ and 250°, most (90%) FVWs have positive velocities, while in the rest, FVWs with negative velocities are dominant (70%). In total, the fraction of FVWs at positive velocities is significantly greater, 70% versus 30%. The distribution of FVWs with positive and negative velocities are also markedly different in their latitude distribution (Fig. 4, *right*): Positive-velocity FVWs are concentrated toward the Galactic plane, although the FWHM is large, while negative-velocity FVWs are roughly uniformly distributed.

The above statistical properties might reflect the detectability of FVWs in the first place, e.g., how smooth and sharp the boundary of the general Galactic H I emission is in the (ℓ, v) diagram. In the first and second quadrants, the boundaries at negative velocities (hereafter negative boundaries), which correspond to the edge of the Galaxy, are wiggly and diffuse, so identification of negative FVWs are difficult there. In addition, anticenter shell (ACS) and HVC complexes make negative boundaries in the second quadrant complicated (Table 1). The boundaries at positive velocities (hereafter positive boundaries) are generally smooth and sharp, although they become complicated toward the inner Galaxy, particularly between $\ell \approx 0°$ and $\sim$30°, where there is not much ISM and the gas motion is not circular. The above explains why most of the FVWs in the first and second quadrants have positive velocities and also why there are relatively few FVWs in the innermost Galaxy. In the third and fourth quadrants, it is negative boundaries that are smooth and sharp. But they are not as sharp as the positive boundaries in the first and second quadrants. In addition, ACS makes the negative boundaries at $\ell \approx 180°$–200° complicated. This may explain why the negative-velocity FVWs in these quadrants are not as dominant as the positive-velocity FVWs in the first and second quadrants.

On the other hand, there is no reason for positive-velocity FVWs at $\ell = 130°$–180° to be more difficult to be identified than those at $\ell = 80°$–120° because both areas have very smooth and sharp positive boundaries. Therefore, there should be intrinsically fewer positive-velocity FVWs in this area. In addition, there are no obvious changes in boundary shapes to cause the asymmetry and the broad extent in latitude distribution.

Figure 5 shows the distribution of column density of FVWs. About 90% of FVWs have values $N_{\rm H} \lesssim 8 \times 10^{19}$ cm^{-2}. The median $N_{\rm H}$ is 2.8×10^{19} cm^{-2}. Note that this is the column density over the velocity interval in Table 2.

3.3. *Comparison with Other Known Objects*

We compared the positions of FVWs with those of SNRs, nearby galaxies, and HVCs, and we found that 6, 4, and 3 FVWs are coincident with those objects, respectively.

For comparison with SNRs, we used Green's SNR catalog (Green 2006). We have found 6 FVWs coincident with SNRs and the results are summarized in Table 3. Systematic studies to search for high-velocity H I gas have been made toward 200 SNRs (Koo & Heiles 1991; Koo et al. 2004). They identified 25 SNRs with fast-moving H I gas localized on SNR areas. Five SNRs out of 25 are identified as FVWs in this paper, i.e., FVWs in Table 3, excluding FVW 112.0−2.0, which is coincident with Cas A. The other 20 SNRs are not identified as FVWs due for several reasons. Some SNRs' expansion velocities are not large enough to be identified as a FVW in a large-scale (ℓ, v) diagram. Some have small size so that their excess emission at high velocities are smoothed out in the data with low angular resolution. For three SNRs in Table 3, high-resolution studies of the shocked H I gas have been made previously, e.g., W51 by Koo & Moon (1997), CTB80 by Koo et al. (1990), and DR4 by Braun & Strom (1986). We have detected FVW toward Cas A, but, considering that Cas A is only $\sim$300 yr old, it seems to be a chance coincidence. The spectrum of the Cas A region is very noisy due to strong radio continuum.

For comparison with galaxies, we used the Nearby Galaxies Catalog of Tully (1988), which includes 2367 galaxies with systemic velocities less than 3000 km s^{-1}. Three FVWs are identified as galaxies according to this catalog. Another FVW, FVW 94.5+8.0, looks similar to those 3 FVWs and turned out to be a

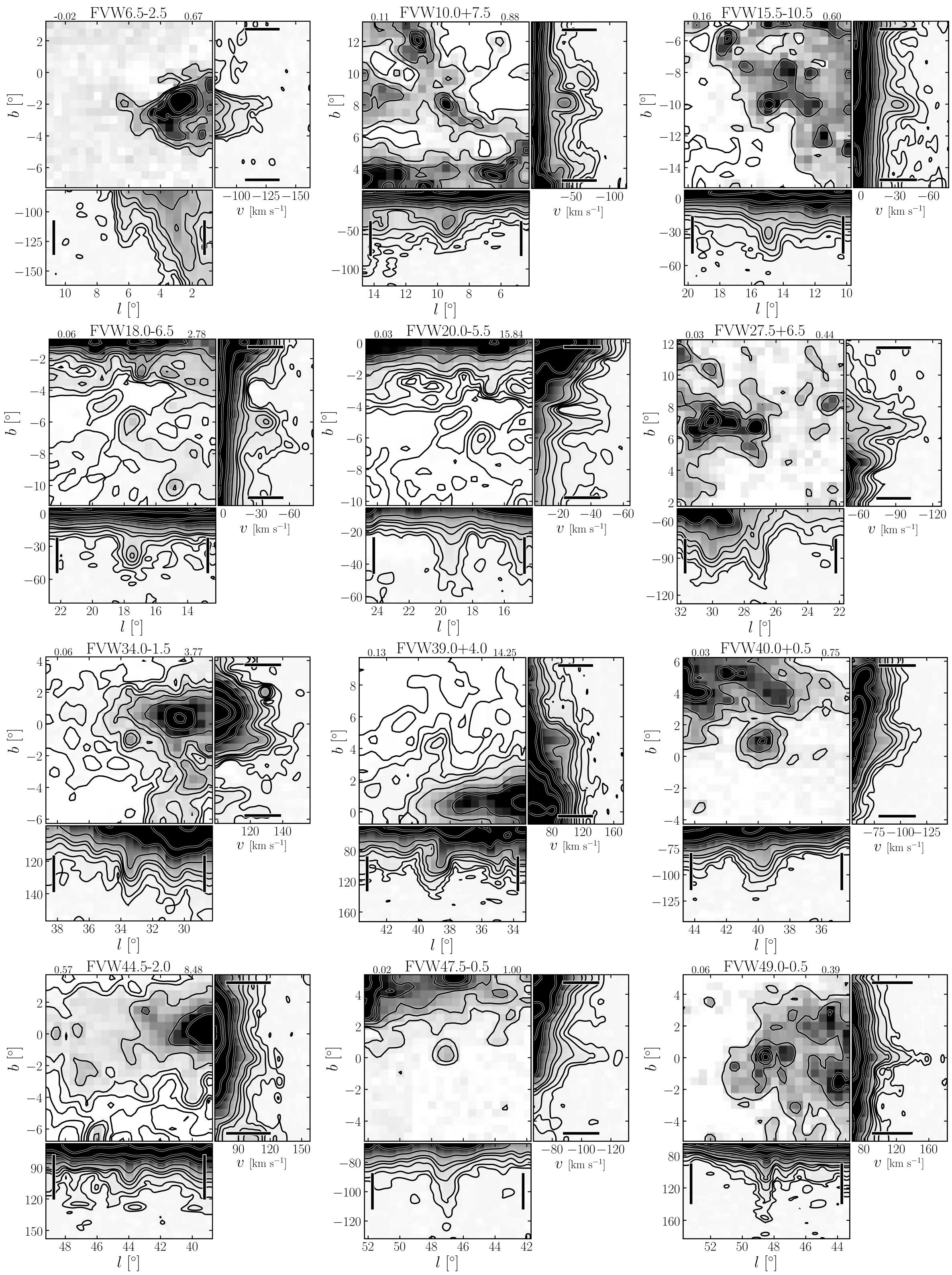

FIG. 2.—FVW's integrated image and its (ℓ-v) and (b-v) diagrams are presented at the center, bottom, and right. The integrated velocity range is shown as thick black lines in its position-velocity diagrams. The minimum and maximum values of contours in the integrated map in K km s^{-1} are noted on the left and right side of the FVW name at the top, respectively. The (ℓ-v) and (b-v) diagrams are cut at the longitude or the latitude of the FVW name, except FVW 109.5+2.5 and FVW 197.0+7.0, for which the slicing latitudes are marked in the figure. The contour levels of position-velocity diagrams are 0.1, 0.2, 0.4, 0.7, 1, 2, 5, 10, 30, 50, and 100 K in brightness temperature.

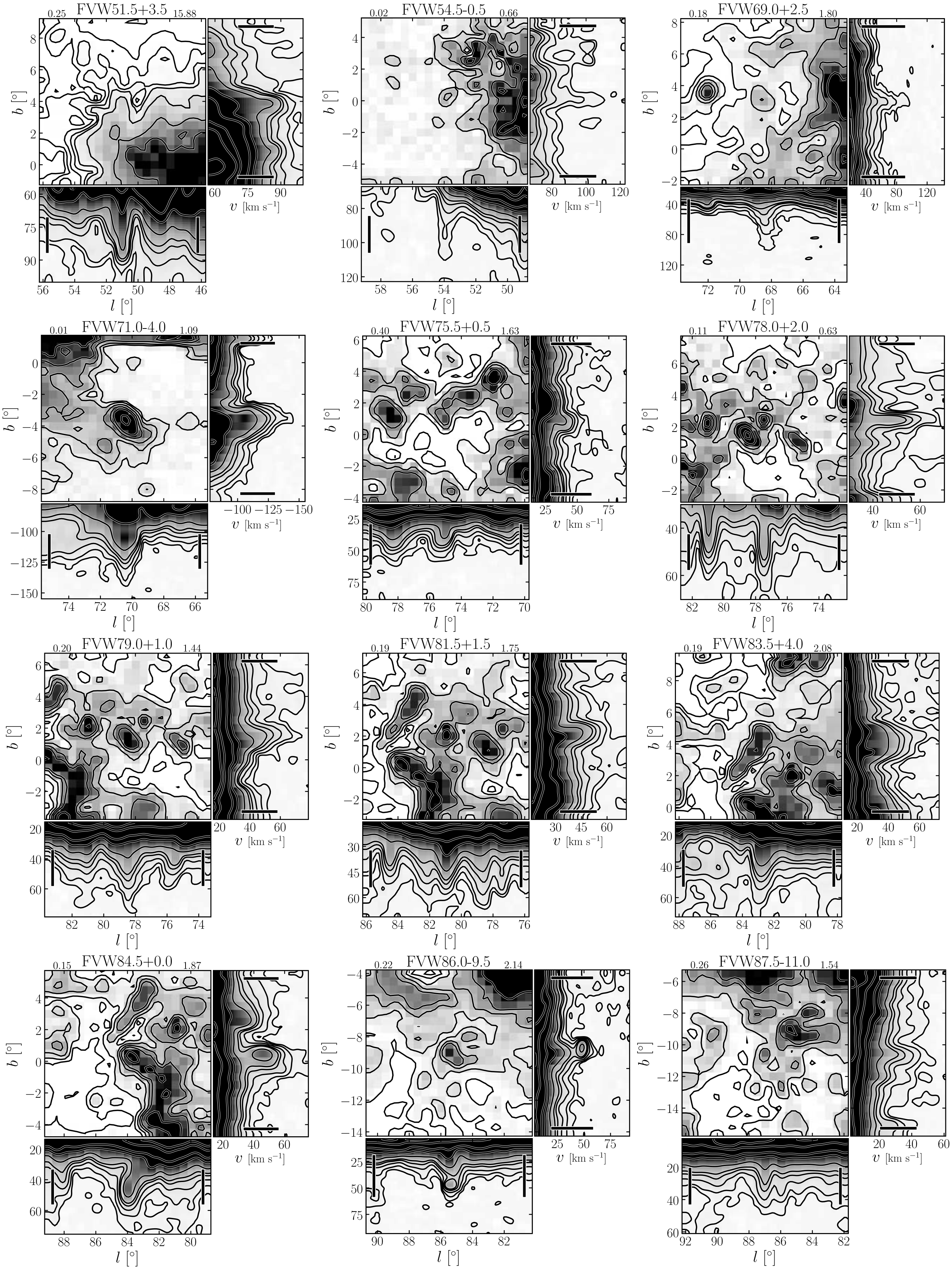

FIG. 2—*Continued*

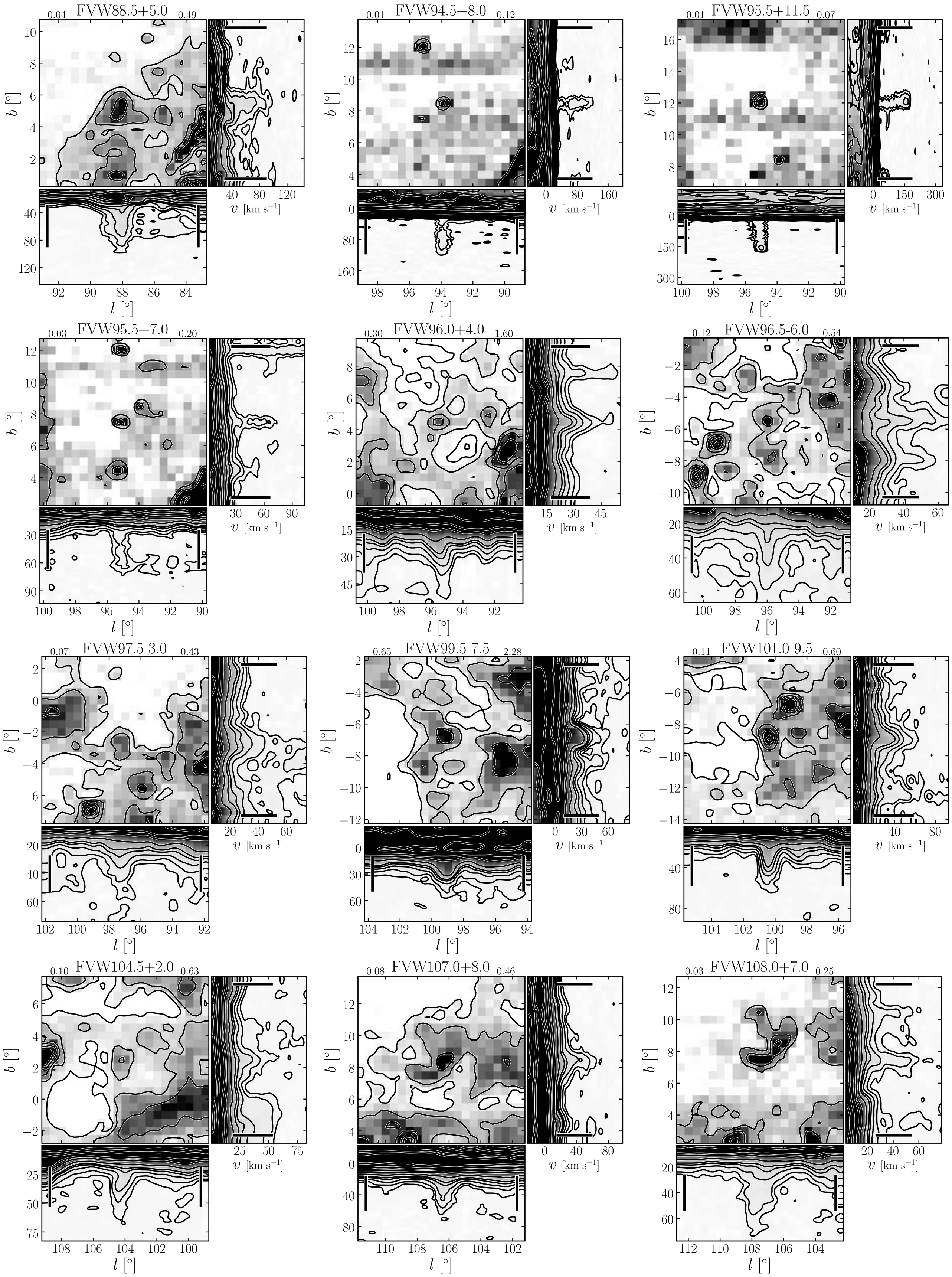

FIG. 2—*Continued*

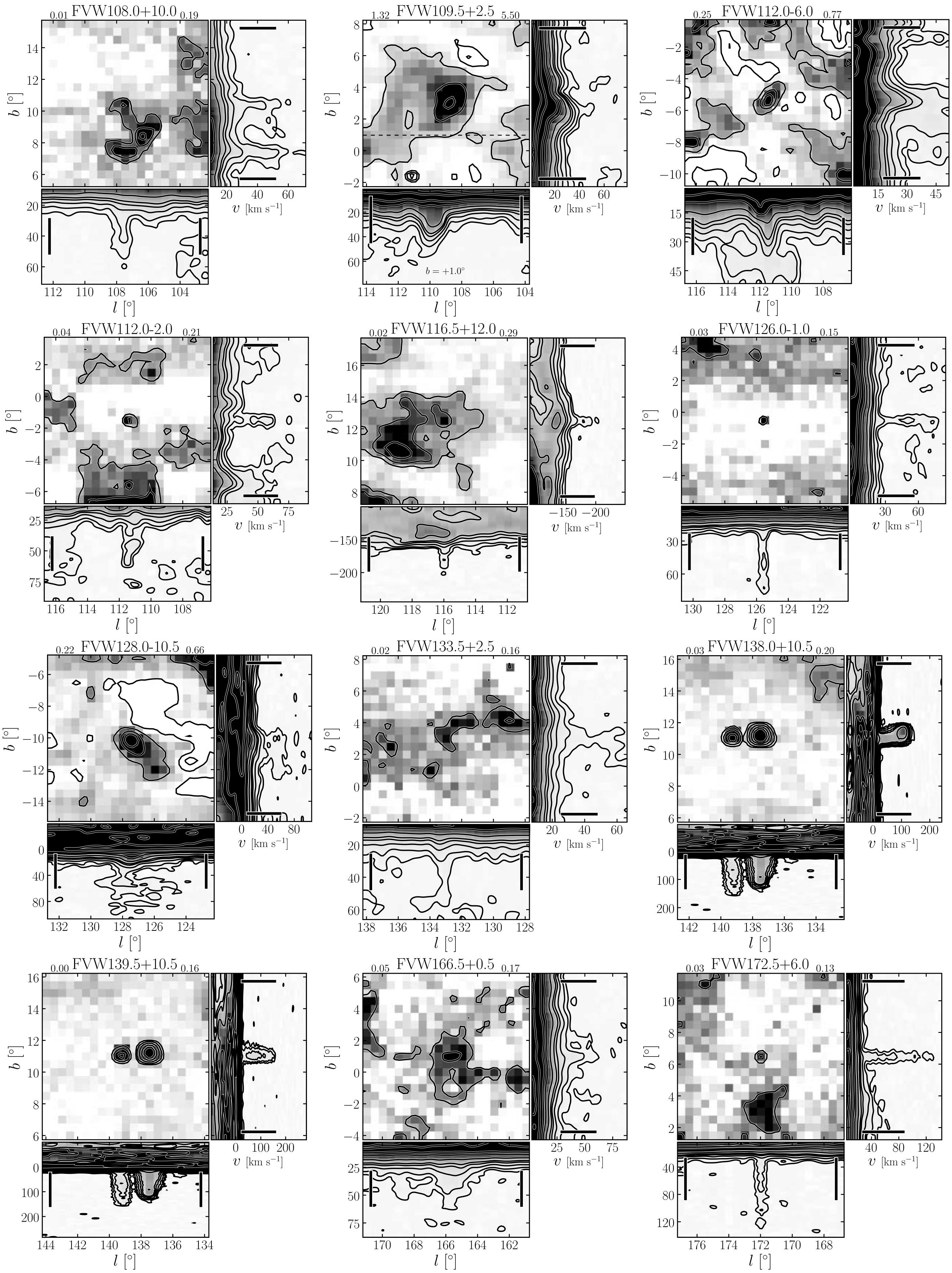

FIG. 2—*Continued*

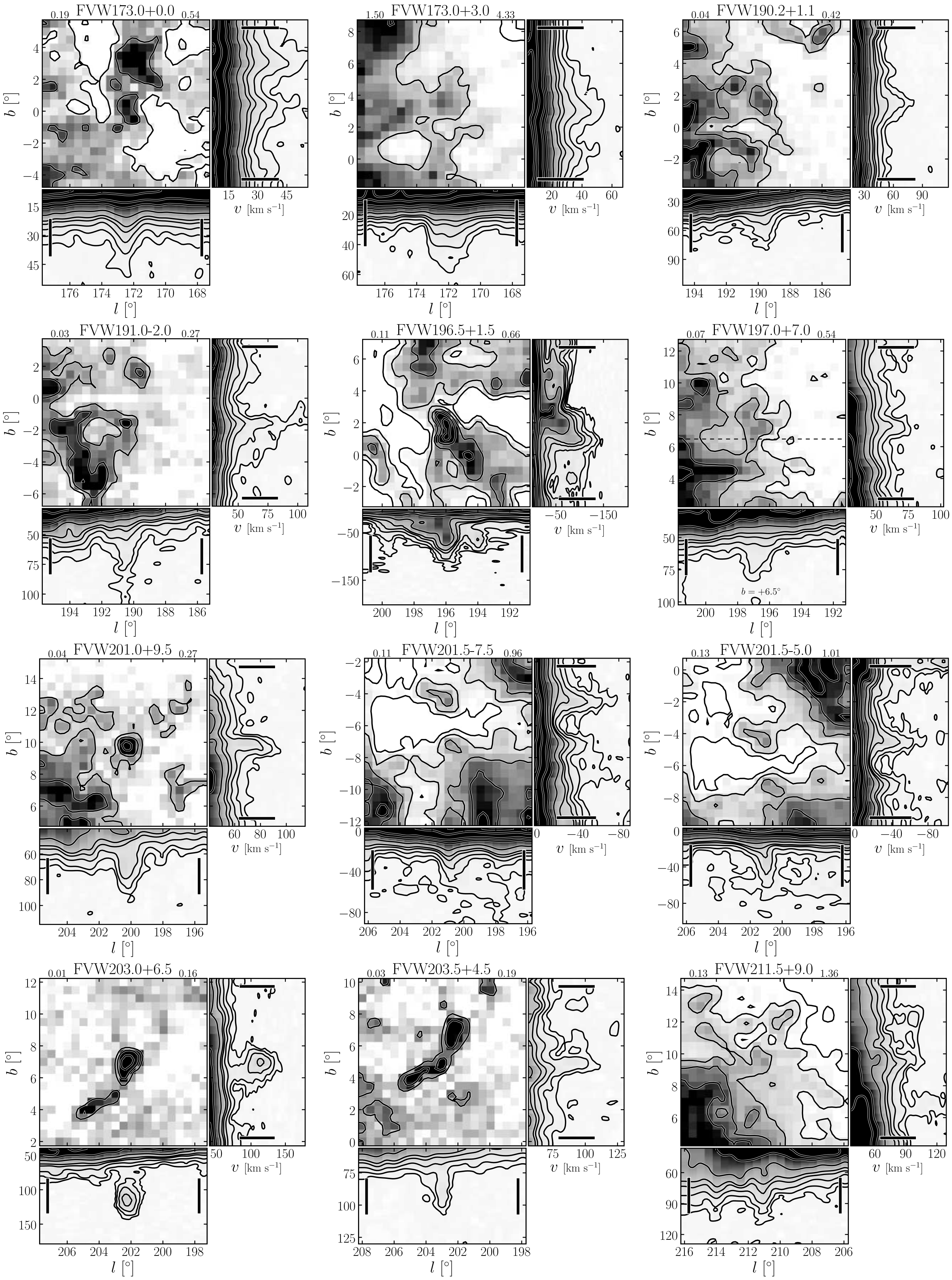

FIG. 2—*Continued*

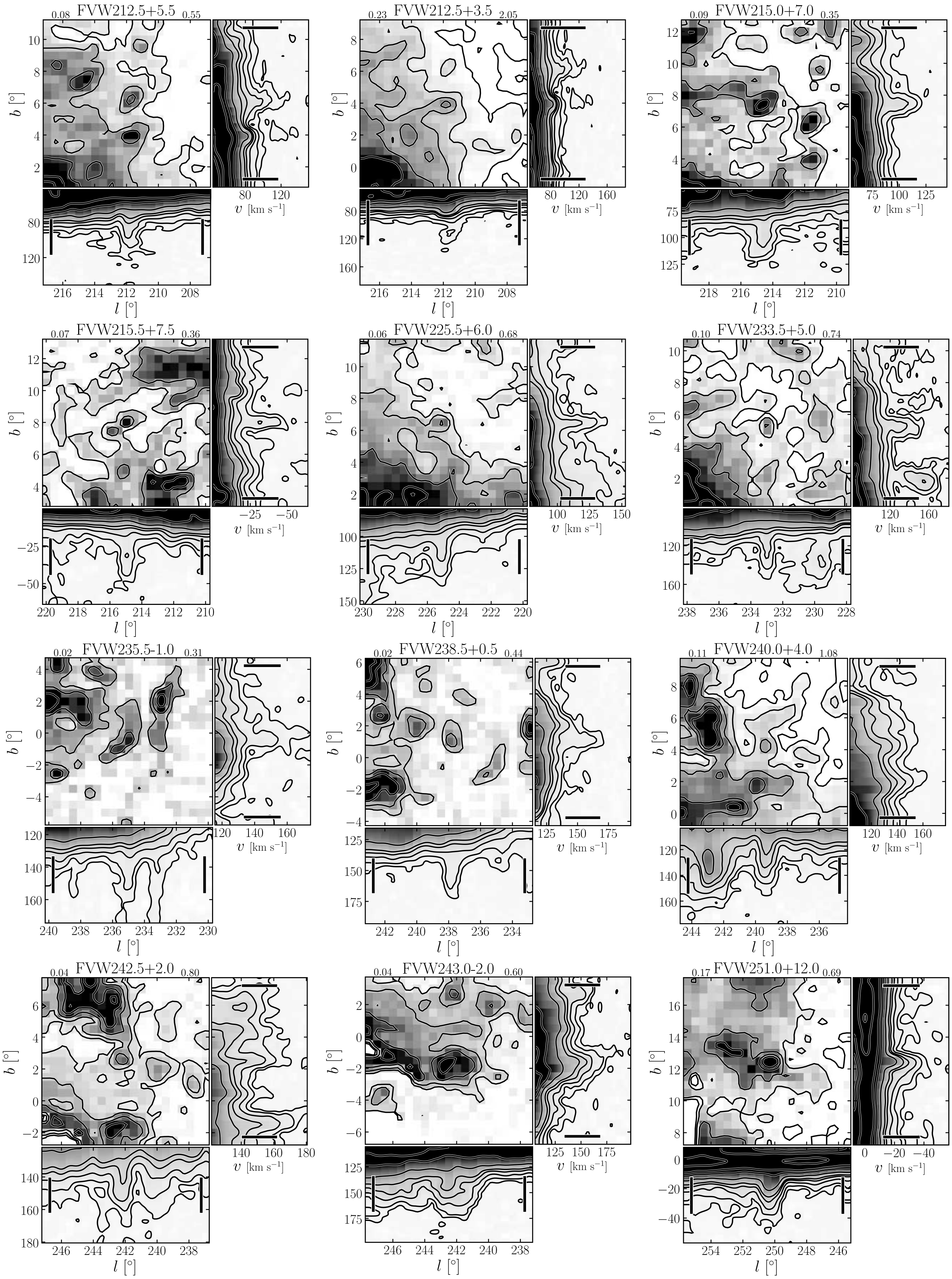

FIG. 2—*Continued*

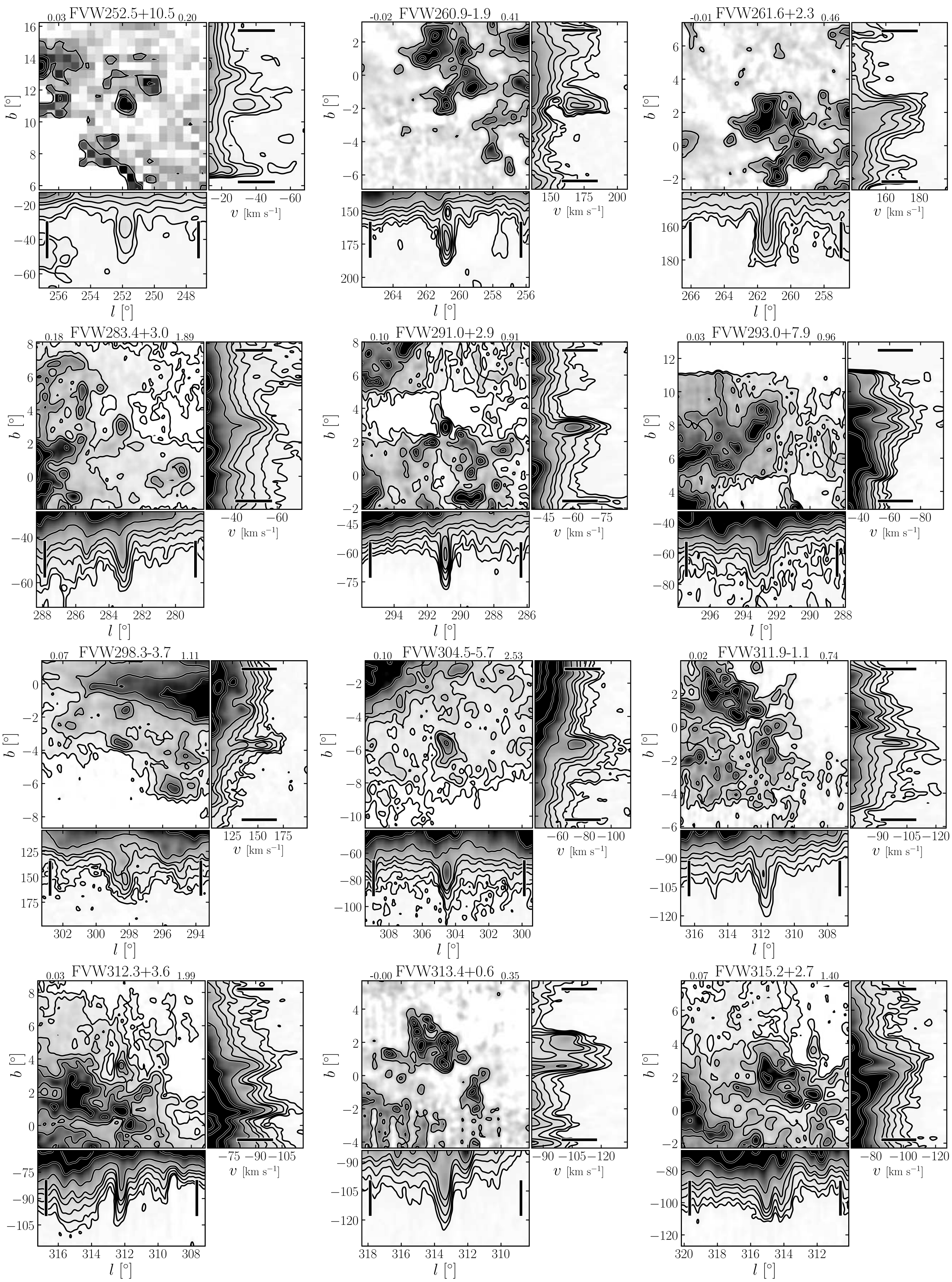

FIG. 2—*Continued*

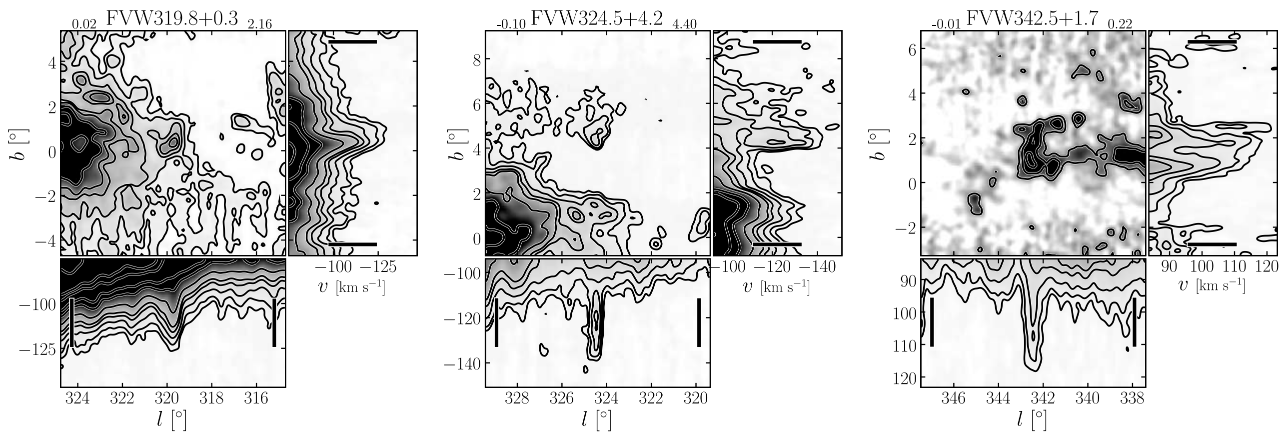

FIG. 2—*Continued*

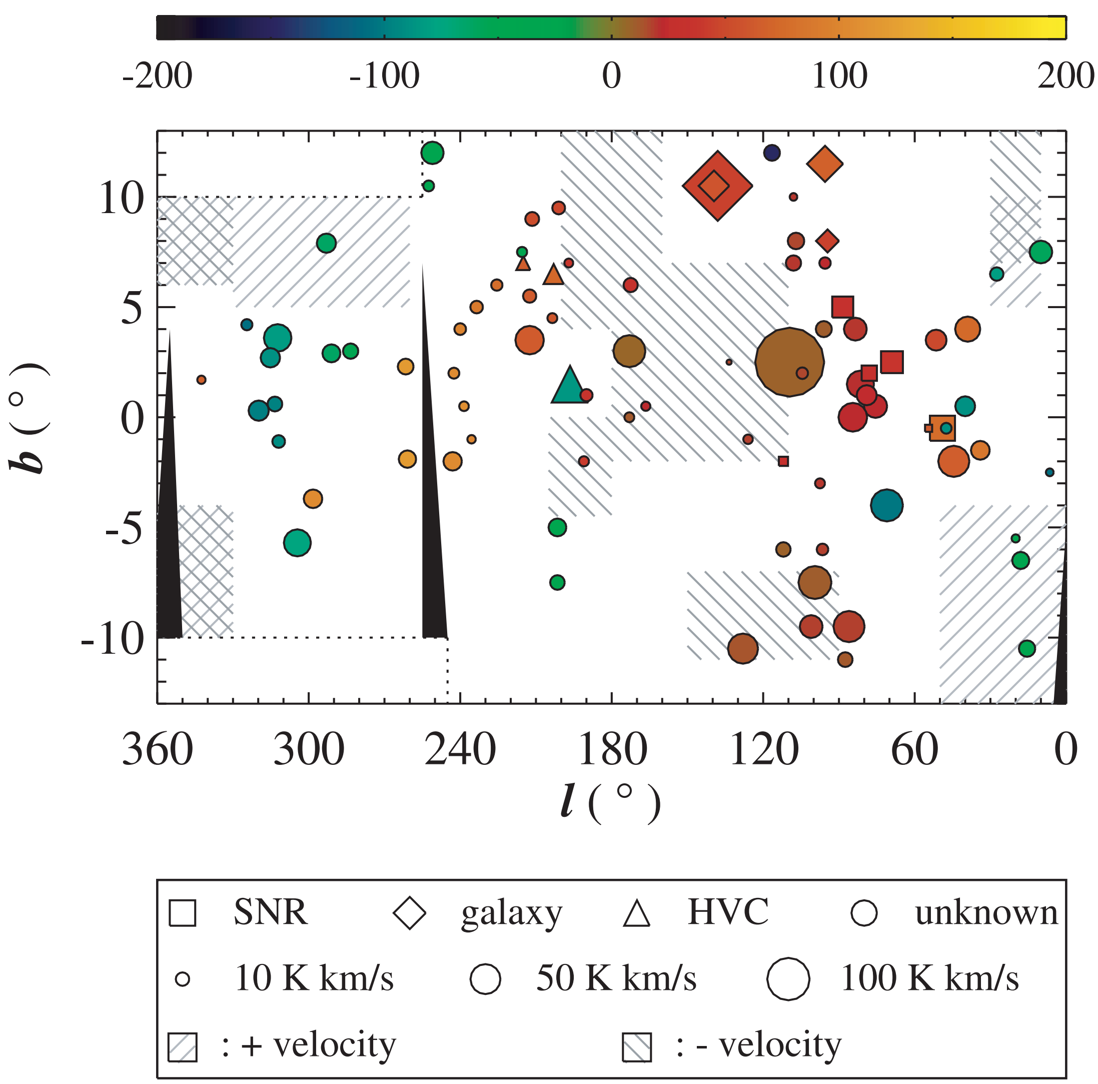

FIG. 3.—Distribution of FVWs in the (ℓ, b) plane. The color of each symbol indicates the mean velocity of the excess emission and corresponds to the velocity in the color bar on the top in km s^{-1}. Each symbol indicates related object, and its occupied area indicates the integrated antenna temperature as shown in the bottom. The hatched areas represent the highly complicated areas in Table 1. The areas filled with solid black show gaps between data, and the dotted line shows the boundary of the search in latitude.

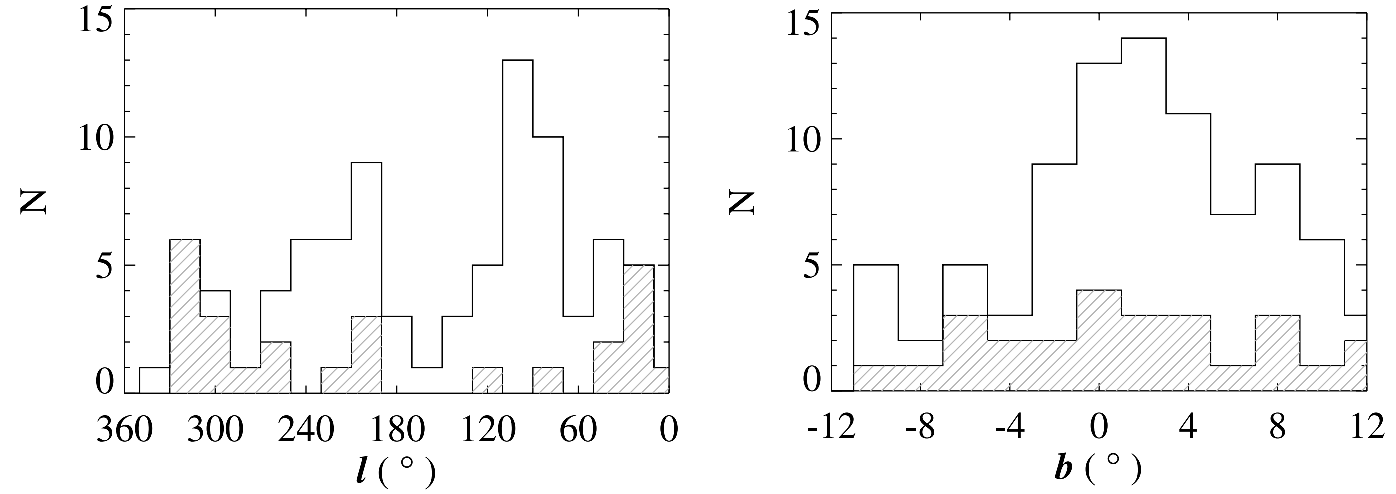

FIG. 4.—*Left*: Distribution of FVWs in Galactic longitude. The hatched area shows the FVWs at negative velocities, while the white area indicates those at positive velocities. *Right*: Same as the left panel, but for Galactic latitude.

low surface brightness galaxy named Cep 1 (Burton et al. 1999). Their parameters are summarized in Table 4. FVWs associated with galaxies have velocity extents wider than 80 km s^{-1} and are easily distinguishable from other FVWs. FVW 172.5+6.0 also shows its excess emission over wide velocity extents comparable to those of galaxies. There is indeed a galaxy named "LEDA 2126032" toward this direction according to the SIMBAD astronomical database. The galaxy has a half-light radius of $\sim 3''$ (2MASS Extended Source Catalog), and its radial velocity is not known. If it is a dwarf galaxy having typical physical half-light radius of 100 pc, it would be at 6 Mpc. Its association with FVW 172.5+6.0 is possible. No other FVWs appear to be external galaxies.

For comparison with HVCs, we used the HVC catalogs of Wakker & van Woerden (1991) including about 560 HVCs of all sky, and Wakker (2001) containing summary catalog based on the absorption line study for the HVCs and IVCs. In addition, we compared the catalog of FVWs with those of compact isolated HVCs (CHVCs; de Heij et al. 2002a; Putman et al. 2002). de Heij et al. (2002a) identified about 900 CHVCs using LDS in the northern sky, and Putman et al. (2002) identified about 2000 compact and extended HVCs in the southern sky using the H I Parkes All-Sky Survey (HIPASS), which covers LSR velocity range between -700 and $+1000$ km s^{-1} with $15.5''$ spatial resolution and 26 km s^{-1} velocity resolution. As shown in Table 5, three FVWs are identified as HVCs. Although $\sim$30% of FVWs unrelated to the known sources show isolated bumps in their spectra (see § 4.2), most of them are not matched with HVCs in available HVC catalogs.

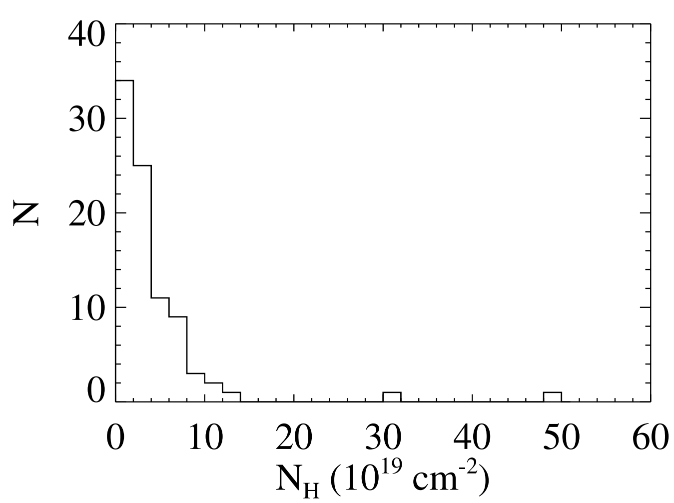

FIG. 5.—Column density distribution of FVWs.

4. DISCUSSION

We have identified 87 FVWs. Among them, 6, 4, and 3 FVWs are found to be coincident with SNRs, nearby galaxies, and HVCs, respectively. The rest (85%) are not associated with any obvious objects that would be responsible for their large velocities. We already pointed out that FVWs associated with galaxies have large, easily distinguishable velocity extents and none of the rest of the FVWs, except perhaps FVW 172.+6.0, seems to be associated with external galaxies. Therefore, FVWs are thought to be Galactic objects. In this section, we discuss possible origins based on their observed properties.

4.1. *Are They SNRs?*

KK04 argued that the number of observed SNRs with H I shells (H I SNRs) is much less than expected and suggested that FVWs could be such missing old SNRs. In fact, in large-scale (ℓ, v) diagrams, the morphologies of most FVWs cannot be discriminated from the FVWs associated with known SNRs. And high-resolution observation showed that at least one FVW, FVW 190.2+1.1, is a rapidly ($\sim$80 km s^{-1}) expanding H I shell that is most likely an old SNR remnant (Koo et al. 2006). Hence, old SNRs are considered to be primary candidates for FVWs.

The distribution of FVWs, however, appears significantly different from either that of the known SNRs or from what we expect for old H I SNRs. The known SNRs are strongly concentrated toward the inner Galaxy and toward the Galactic plane. If we use the 265 SNRs in Green's catalog (Green 2006), the longitude distribution has a maximum at $\ell \approx 10°$ and a FWHM of $\sim 90°$, while the latitude distribution is almost symmetric with a FWHM of $\sim 1°$. The expected distribution of old SNRs identifiable in H I emission had been calculated by KK04 using a simple model where it was assumed that the Galaxy is composed of a uniform, axisymmetric gaseous disk with a central hole and that only Type Ia supernovae produce isolated SNRs that are exponentially distributed with a radial scale length of 3 kpc. According

TABLE 3
FVWs Coincident with SNRs

FVW Name	SNR Parameters: Name	Other Name(s)	Size (arcmin)	Distance (kpc)	Reference
FVW 49.0−0.5	G49.2−0.7	W51	30	4.1	1
FVW 54.5−0.5	G54.4−0.3	HC40	40	3.3	2
FVW 69.0+2.5	G69.0+2.7	CTB 80	80	2.0	3
FVW 78.0+2.0	G78.2+2.1	DR4, γ Cygni SNR	60	1.4	2
FVW 88.5+5.0	G89.0+4.7	HB21	120 × 90	0.8	4
FVW 112.0−2.0	G111.7−2.1	Cassiopeia A, 3C461	5	3.4	5

References.—(1) Sato 1973; (2) Milne 1979; (3) Koo et al. 1990; (4) Uyaniker et al. 2003; (5) Reed et al. 1995.

to their result, visible H I SNRs are concentrated in the inner Galaxy along the loci of tangent points ($\ell \approx 40^\circ$ and 320°) because the SN rate is higher in the inner Galaxy and because the systemic velocities of SNRs in those regions are close to either the maximum or the minimum velocities of the Galactic background emission. The number of visible H I SNRs is ~100, 75% of which is within $|\ell| \leq 70^\circ$. KK04 did not calculate the latitude distribution, but if SN Ia distribution follows thin old stellar disk with an exponential scale height of ~300 pc as in their model, the FWHM of these visible H I SNRs would be ~6°. These results, showing that the expected distribution of visible H I SNRs is quite different from that of FVWs, however, do not necessarily rule out the SN origin for FVWs: First, the number of H I SNRs in the inner Galaxy could be significantly less than that in the model if the interstellar space there is largely filled with a very tenuous gas instead of warm neutral medium (0.14 cm^{-3}), as KK04 pointed out. And, second, in the outer Galaxy, there could be more visible H I SNRs than the model because the identification is relatively easy there. In addition, core-collapse SNe may not be spatially and/or timely correlated in there, so that they result in H I SNRs, too. However, the significantly larger number in the outer Galaxy and their large scale height seem to indicate that not all of FVWs could be old SNRs.

If FVWs are SNRs, it may be possible to see faint radio continuum emission associated with them. We have searched associated radio emission toward 38 FVWs covered in the Effelsburg 11 cm continuum survey (Reich et al. 1990; Fürst et al. 1990) ($0^\circ \lesssim \ell \lesssim 240^\circ$, $|b| \lesssim 5^\circ$). Nine FVWs are found to have noticeable extended emission within a 2° sized circle in addition to the 6 FVWs coincident with the known SNRs (Fig. 6). They are summarized in Table 6. The cases of FVW 173.0+0.0 and FVW 173.0+3.0 are interesting: There is an about a 3° sized, incomplete shell-like continuum feature centered at $(\ell, b) \sim (172.5^\circ, +1.5^\circ)$, and H I emission of FVW 173.0+3.0 appears to be enclosed by the filamentary continuum emission, while FVW 173.0+0.0 lies on the south of the shell-like continuum. Other than these two, there are no obvious coincident shell-like continuum features. In order to prove the association of these radio features with FVWs, further studies are required.

4.2. *Anomalous Velocity Clouds*

About 30% of FVWs unrelated to known SNRs, galaxies, or HVCs show isolated bumps in their spectra, e.g., FVW 15.5−10.5 in Figure 2. They appear as H I 21 cm wings in large-scale (ℓ, v) diagrams because they are very close to the Galactic H I emission. These FVWs therefore could be clouds with anomalous velocities rather than expanding shells. Table 7 lists such FVWs. The FVWs associated with known SNRs, HVCs, or galaxies are not included, even though they show isolated bumps in their spectra. The bumps in some FVWs in Table 7, e.g., FVW 75.5+0.5, FVW 293.0+7.9, and FVW 312.3+3.6, are weak (~1 K) and not apparent in Figure 2 (see the notes in Table 7). On the other hand, there are FVWs that appear to have very weak (~0.2 K), broad bumps in Figure 2, e.g., FVW 95.5+7.0 and FVW 126.0−1.0, but they are hardly identified as isolated bumps in their spectra and not included in Table 7.

We have determined central LSR velocity, FWHM, and brightness temperature of FVWs with isolated bumps by fitting their spectra into a Gaussian plus a second-order polynomial function. Table 7 summarizes the result.

Their central velocities vary from $v_{LSR} = -124.3$ to +170.3 km s^{-1}. Their FWHMs are 7.0–25.5 km s^{-1} with median value of 12.4 km s^{-1}. Their median peak brightness temperature is 1.0 K, and the median hydrogen column density is 2.4×10^{19} cm^{-2}. Table 7 also lists the deviation velocity, which is defined as the excess of central velocity over the minimum or maximum velocities permitted by the Galactic rotation (Wakker 1991). Here we assume a Galactic model that Wakker (1991) used, i.e., a 4 kpc thick disk with radius 26 kpc and a flat rotation curve with a value of $v_\odot = 220$ km s^{-1} and $R_\odot = 8.5$ kpc. The deviation velocities

TABLE 4
FVWs Coincident with Nearby Galaxies

FVW Name	Galaxy Parameters: (ℓ, b) (deg)	Other Name(s)	Size (arcmin)	Velocity[a] (km s^{-1})	Distance (Mpc)	Reference
FVW 94.5+8.0	(94.37, +8.01)	Cepheus 1	11.7	58	6.0	1
FVW 95.5+11.5	(95.72, +11.68)	NBG 2146, NGC 6946	11.2	46	5.5	2
FVW 138.0+10.5	(138.18, +10.58)	NBG 329, UGC 2847	16.1	32	3.9	2
FVW 139.5+10.5	(139.77, +10.64)	NBG 348, UGCA 86	1.0	72	4.4	2

[a] Heliocentric systematic velocity.
References.—(1) Burton et al. 1999; (2) Tully 1988.

TABLE 5
FVWs Coincident with HVCs

	HVC Parameters				
FVW Name	(ℓ, b) (deg)	Size (deg)	Velocity (km s^{-1})	$N_{\rm H}$ (10^{18} cm^{-2})	Reference
FVW 196.5+1.5......	(197.0, +1.5)	~1.0	−66.0	100	1
FVW 203.0+6.5	(202.8, +6.4)	2.5	108.4	120	2
FVW 215.0+7.0......	(215.0, +7.0)	1.1	103.0	50	2

References.—(1) Wakker 2001; (2) Wakker & van Woerden 1991.

range from −33.8 to +46.6 km s^{-1}, and the median value is 31.9 km s^{-1}. The negative $v_{\rm dev}$ means that the central velocity is within the allowed velocity range, which implies that the used disk model does not describe well the real velocity boundaries.

The velocities of FVWs indicate that they could have been classified either as HVCs or IVCs. HVCs are generally defined as clouds with velocities greater than 90 km s^{-1} with respect to the local standard of rest (LSR; Wakker 2001; Putman et al. 2002). At low Galactic latitudes, however, this definition is not very useful and an alternative definition in terms of the deviation velocity could be used, i.e., $v_{\rm dev} \gtrsim 50-60$ km s^{-1} (Wakker 1991;

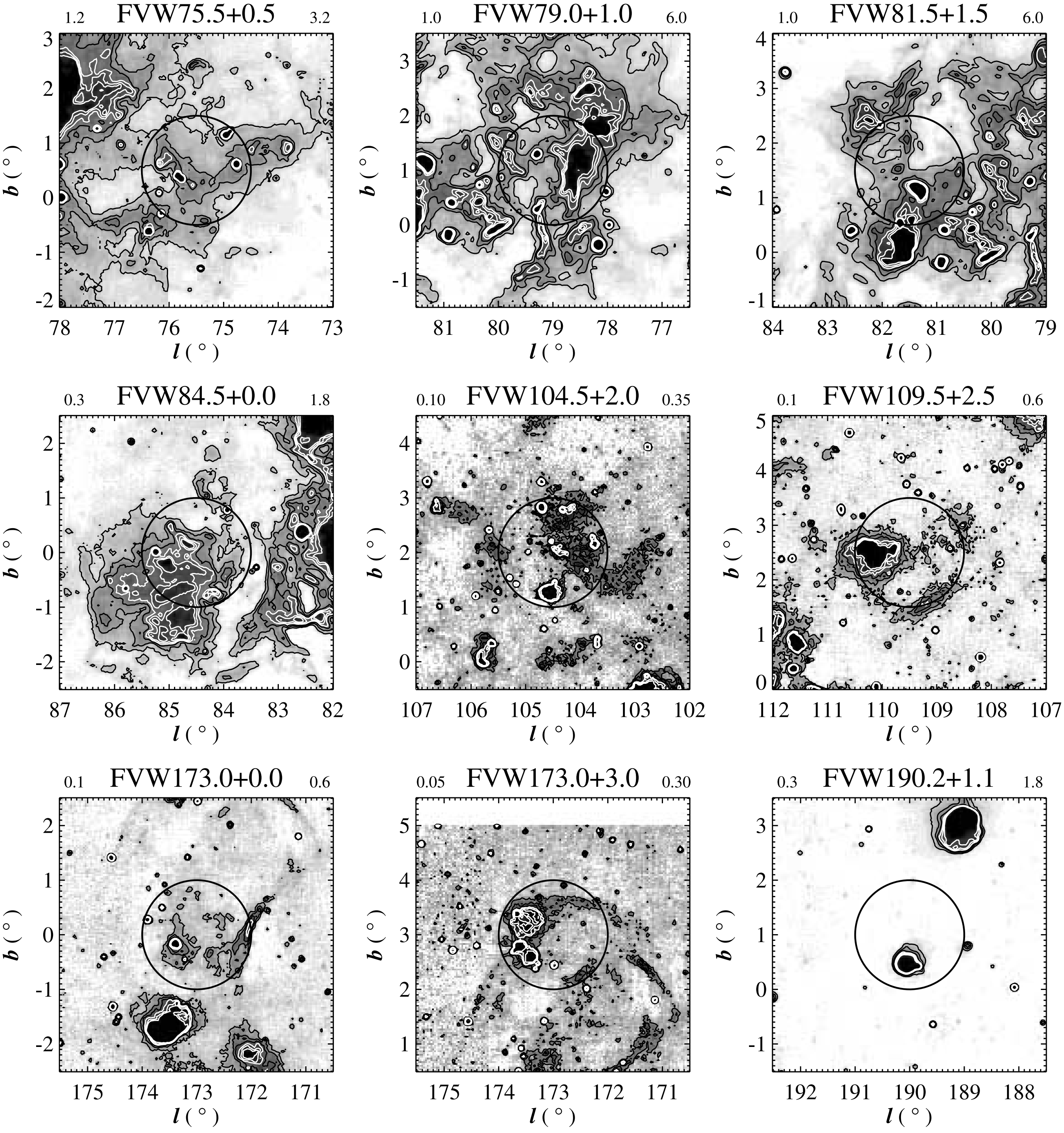

Fig. 6.—Effelsberg 11 cm continuum images of 9 FVWs having noticeable extended emission. The minimum and the maximum contour levels in brightness temperature (K) are written at the top left and the top right corner of the image. Contours are equally spaced. The gray image and the contours are focused on showing faint emission. The circle at the center represents area within diameter of 2°.

TABLE 6

FVWs with Coincident Radio Continuum Emission

FVW Name	Radio Continuum Characteristics
FVW 75.5+0.5	Extended feature, not well matched with H I
FVW 79.0+1.0	Complicated area
FVW 81.5+1.5	Complicated area
FVW 84.5+0.0	Complicated area
FVW 104.5+2.0	H II region, not well matched with H I
FVW 109.5+2.5	H II region, not well matched with H I
FVW 173.0+0.0	3° sized filamentary shell-like feature
FVW 173.0+3.0	Part of 3° sized filamentary shell-like feature
FVW 190.2+1.1	H II region, not well matched with H I

Putman et al. 2002). Observationally IVCs are just lower velocity counterparts of HVCs, which are defined as clouds with 30–40 km s^{-1} $\lesssim |v_{\rm LSR}| \lesssim$ 90 km s^{-1} (Wakker 2001; Richter et al. 2003) in terms of LSR velocity. About one-third of the FVWs in Table 7 have central LSR velocities $|v_{\rm LSR}| = 100$–170 km s^{-1}, so they may be classified as HVCs while the rest are classified as IVCs. On the other hand, all of them have deviation velocities less than 50 km s^{-1}, which puts them in the category of IVCs. An interesting feature of HVCs is that they show a systematic velocity change, i.e., most HVCs are at positive velocities between $\ell \sim 200°$ and 320°, while most of them are at negative velocities in the rest (Wakker & van Woerden 1991). This asymmetric velocity structure was explained by a model where HVCs are debris of the parental cloud of the Local Group, falling toward the center of the Local Group (Blitz et al. 1999; de Heij et al. 2002b). The FVWs in Table 7 show somewhat opposite velocity trend, i.e., about 70% of FVWs between $\ell \sim 200°$ and 320° are at negative velocities, which is similar to the trend of the entire FVWs (§ 3.2). This makes it difficult to consider the FVWs as a low-velocity population of HVCs.

It is also possible that the FVWs with isolated bumps are small, fast-moving clouds unresolved in the survey. Recently, small ($\lesssim$10 pc), fast-moving clouds are revealed by high-resolution observations in the disk/halo interface region of the inner Galaxy, so-called halo clouds (Lockman 2002), in the disk ($|b| < 1.3°$) of the inner Galaxy (Stil et al. 2006), and in the anticenter region (Stanimirović et al. 2006). It was suggested that our Galaxy may possess a population of those clouds distributed both throughout the disk and up into the halo rotating with the Galactic disk and that about one-half of the Galactic H I halo could be in the form of discrete clouds (Lockman 2002; Stil et al. 2006). They could be clouds formed in Galactic fountain flows or infalling intergalactic material in the ongoing construction of the Galaxy (Stanimirović et al. 2006 and references therein). The observational properties of the halo clouds and the clouds in the inner Galactic disk and in the anticenter region are summarized by Stanimirović et al. (2006, their Table 3). The properties of FVWs in Table 7 are quite comparable to those of halo clouds, i.e., their velocity dispersion (12 km s^{-1}) and H I column densities (2×10^{19} cm^{-2}) are similar. The fast-moving clouds in the inner Galactic disk have a factor of 2 smaller FWHM and much larger H I column densities, while the clouds in the anticenter region have comparable H I column densities but a factor of 3 smaller FWHM. However, since FVWs are not resolved, this comparison should be considered as provisional until high-resolution maps of FVWs are available.

We should keep in mind that the isolated bump in spectrum does not necessarily mean that a FVW is not part of a SNR. Because the ISM is not uniform, the accelerated H I shells of SNRs often show bumplike features in their H I spectra (e.g., Koo et al. 1990). It is also worth noting that the fast-moving small clouds

TABLE 7

FVWs with Isolated Bumps in Position-Velocity Maps

FVW Name	$v_{\rm center}$[a] (km s^{-1})	$v_{\rm dev}$[b] (km s^{-1})	FWHM[a] (km s^{-1})	Peak T_b[a] (K)	$N_{\rm H\,I}$[c] (10^{18} cm^{-2})	Note
FVW 10.0+7.5	−43.6	20.3	16.6	1.5	50.3	1
FVW 15.5−10.5	−34.1	12.4	13.8	0.7	19.9	1
FVW 18.0−6.5	−39.3	−6.2	12.9	0.9	23.4	1
FVW 71.0−4.0	−105.9	−33.8	7.2	2.5	35.5	1
FVW 75.5+0.5	38.4	31.4	8.1	0.9	13.6	2
FVW 84.5+0.0	45.6	44.5	12.2	2.8	65.8	1
FVW 86.0−9.5	46.9	46.4	5.0	1.8	17.8	3
FVW 201.0+9.5	72.3	20.0	17.0	0.4	14.4	1
FVW 252.5+10.5	−34.4	34.4	8.9	0.4	6.3	1
FVW 260.9−1.9	170.3	24.2	25.5	1.6	82.5	1
FVW 261.6+2.3	164.0	17.6	19.1	0.9	32.7	1
FVW 283.4+3.0	−47.3	41.3	7.0	0.9	11.7	2
FVW 291.0+2.9	−61.2	46.6	11.2	2.4	52.2	1
FVW 293.0+7.9	−56.7	39.4	10.1	1.0	20.7	2
FVW 298.3−3.7	154.5	24.4	11.2	0.6	13.3	4
FVW 304.5−5.7	−76.6	38.1	14.1	1.9	51.6	1
FVW 311.9−1.1	−100.8	44.6	12.3	0.6	14.5	1
FVW 312.3+3.6	−82.3	25.2	12.5	1.2	30.4	2
FVW 313.4+0.6	−102.6	42.5	12.4	1.0	24.2	1
FVW 324.5+4.2	−124.3	32.3	22.4	0.9	39.3	1
Median Values	−41.5	31.9	12.4	1.0	23.8	

Notes.—(1) It is a well-defined, isolated clump. (2) The excess emission is weak in comparison to the Galactic H I, so that the spectral bump is not apparent in Fig. 2, although it is clear in the spectrum. (3) As seen in Fig. 2, FVW 86.0−9.5 consists of smoothly extended H I emission and small clump at higher velocity. The parameters listed in this table are the Gaussian fitting results of the small clump. (4) It shows double bumps in spectrum. The parameters are those of the larger bump.

[a] Values of $v_{\rm center}$, FWHM, and peak T_b were derived by Gaussian fitting.

[b] The variable $v_{\rm dev}$ is defined as the excess of central velocities over the minimum and maximum velocities permitted by the Galactic differential rotation. Thus, negative $v_{\rm dev}$ represents $v_{\rm center}$ is within the velocity range permitted by the given disk model.

[c] Value of $N_{\rm H\,I}$ is derived from the total integrated intensity of Gaussian component.

TABLE 8
FVWs Coincident with Galactic O-Type or WR Stars

FVW Name	Number of Stars[a]	Parameters of the Nearest Star: (ℓ, b) (deg)	Other Names	Spectral Type	Angular Distance (deg)	Distance (kpc)
Galactic O Stars						
FVW 6.5−2.5	2	(6.9, −2.1)	HD 165921	O7.5 V	0.58	1.3
FVW 15.5−10.5	1	(15.3, −10.6)	HD 175876	O6.5 III	0.22	2.3
FVW 75.5+0.5	6	(75.9, +0.8)	HD 193682	O5. V	0.50	1.8
FVW 79.0+1.0	4	(79.0, +1.3)	BD +40 4179	O8. V	0.30	1.2
FVW 83.5+4.0	1	(83.8, +3.3)	BD +45 3216	O8.	0.77	1.9
FVW 104.5+2.0	1	(103.8, +2.6)	HD 210839	O6. I	0.92	0.8
FVW 109.5+2.5	5	(109.6, +2.7)	HD 216532	O9.5 V	0.21	0.9
FVW 173.0+0.0	4	(173.0, +0.1)	HD 35619	O7. V	0.10	3.2
FVW 173.0+3.0	3	(173.5, +3.2)	HD 37737	O9.5 III	0.54	1.3
FVW 190.2+1.1[b]	1	(190.0, +0.5)	HD 42088	O6.5 V	0.50	1.5
FVW 313.4+0.6	3	(313.5, +0.2)	HD 125241	O8.5 I	0.47	3.2
FVW 342.5+1.7	9	(342.8, +1.7)	HD 151515	O7. III	0.30	1.9
Galactic WR Stars						
FVW 75.5+0.5	3	(75.7, +0.3)	Sand 5	WO2	0.30	0.9
FVW 79.0+1.0	2	(79.7, +0.7)	V1923 Cyg, AS 422	WN7/WCE+?	0.77	
FVW 342.5+1.7	1	(343.2, +1.4)	HD 151932	WN7h	0.77	2.0

Notes.—All parameters of the nearest star in this table are from Garmany et al. (1982) or van der Hucht (2001) except angular distance, which simply indicates angular distance of the nearest star from a FVW center. Distance of HD 151932 leaves blank since it is not noted in the reference catalog.

[a] Number of stars in 1° radius.

[b] High-resolution study of Koo et al. (2006) revealed that FVW 190.2+1.1 is possibly old SNR and not quite related with HD 42088.

usually appear related to diffuse filamentary structures (Stanimirović et al. 2006), which suggests a possibility of disrupted SNR shells. The nature of those cloudlike FVWs needs further study.

4.3. *Other Possibilities*

Another candidate for FVWs is stellar winds and wind-blown shells. Low- and high-mass protostars produce quickly expanding winds or jets. OB stars or Wolf-Rayet (WR) stars eject strong winds forming expanding ionized or neutral H I shells. AGB stars also expel their energies into the surrounding medium as slow and fast winds. Here we will discuss if they could be detectable in the H I surveys used in this work.

Low- and high-mass protostars lose their masses by stellar winds and jets. The wind could be neutral intrinsically (Lizano et al. 1988) or neutral hydrogen could be produced by dissociation of molecular hydrogen in shocks (Bally & Stark 1983). Neutral atomic stellar wind was detected toward the young stellar object HH 7-11 at 350 pc from the Sun (Lizano et al. 1988). The average antenna temperature of neutral wind of the HH 7-11 is ~0.01 K when it is observed at the Arecibo telescope. This corresponds to an antenna temperature of $\lesssim$0.001 K for a 25 m or 64 m telescope. Therefore, if the observed parameters of HH 7-11 represent typical wind parameters of low-mass protostars, FVWs identified in this paper ($T_A \gtrsim 0.1$ K) cannot be due to such neutral winds.

Neutral atomic stellar wind has been detected toward high-mass protostars, too. Russell et al. (1992) detected atomic stellar wind expanding at ~90 km s^{-1} toward DR 21, which contains one of the most powerful outflow sources in the Galaxy. The H I mass of the wind is 24 $M_\odot$ at the generally accepted distance of DR 21 (3 kpc), which is 3 orders of magnitude more massive than the H I wind seen in HH 7-11. This would yield ~0.007 K for a 25 m telescope. If we assume the observed parameters of DR 21 is typical, the neutral winds from massive protostars would not be detectable unless they are closer than $\lesssim$1 kpc.

Strong stellar wind from early type OB stars or WR stars is likely to be an another possible source producing fast-moving H I gas. The mechanical luminosity of winds from OB stars range from 10^{31} to 10^{37} ergs s^{-1} with a typical expansion velocity of 1500 km s^{-1} (Bieging 1990). This wind sweeps up ambient medium into a shell that could be observed as FVWs. Most observed H I shells around OB stars, however, have low expansion velocities, i.e., $\lesssim$20 km s^{-1} (e.g., Cappa & Herbstmeier 2000; Cappa et al. 2002; Boulva 1999). But these expansion velocities might be lower limits because their endcaps are not usually detected. According to Weaver et al. (1977) the radius of the expanding shell is given by $R(t) = 26 n_0^{-0.2} L_{36}^{0.2} t_6^{0.6}$ pc, where n_0 is ambient atomic density of H nuclei in cm^{-3}, L_{36} is the wind luminosity in 10^{36} ergs s^{-1}, and t_6 is the age in 10^6 yr. From this, we may express the mass in the shell $M(t)$ in terms of its expansion velocity $v(t)$; $M(t) = (4\pi/3)\rho_0 R(t)^3 = 0.4 n_0^{-0.5} L_{36}^{1.5} v_2^{-4.5}\, M_\odot$, where v_2 is expansion velocity in 100 km s^{-1}. When this shell is observed with a 25 m telescope, it would yield a brightness temperature of $T_b \simeq 0.6 M(t) d^{-2} \Delta v^{-1}$, where $M(t)$ is in $M_\odot$, d is the distance in kpc, and Δv is the velocity interval over which the H I shell would be detected in km s^{-1}. Since 0.1 K is a detection limit in this work, the ones at distance less than $d \lesssim 0.11 n_0^{-0.25} L_{36}^{0.75} v_2^{-2.75}$ kpc could be detected assuming $\Delta v \simeq 2v(t)$. If we assume that the shells of expansion velocity $v(t) \gtrsim 50$ km s^{-1} are detectable, then the distance should be less than $d \lesssim 0.7 n_0^{-0.25} L_{36}^{0.75}$ kpc. Thus, nearby ($\lesssim$4 kpc) wind shells with large wind luminosity ($\gtrsim 10^{37}$ ergs s^{-1}) can be detected, assuming $n_0 \simeq 1$ cm^{-3}.

We checked whether O-type or Wolf-Rayet stars having large wind luminosities are in the region of FVWs, using the Galactic O star catalog of Garmany et al. (1982) and the seventh catalog of Galactic Wolf-Rayet stars of van der Hucht (2001). About 15% of FVWs unrelated to the known sources have more than one stars in 1° radius area. They are summarized in Table 8. Twelve and three FVWs have nearby O stars and WR stars, respectively. All

3 FVWs coincident with WR stars are coincident with O stars, too. They are at quite close distance ($d \lesssim 3$ kpc). Thus, some of those FVWs in Table 8 could be caused by winds from massive stars. However, it is worthy to note that the FWHM of the latitude distribution of early type stars ($\sim 1°$) (Paladini et al. 2003) is much smaller than that of FVWs ($\sim 13°$).

Highly evolved cool stars in asymptotic giant branch (AGB) eject strong stellar winds too and could be an another candidate for FVWs. For example, molecular outflow at a speed of ~ 200 km s^{-1} has been detected in AGB carbon star V Hya (Knapp et al. 1997). These molecular winds may collide with the interstellar medium to produce fast-moving atomic gas. In particular, the FWHM of the latitude distribution of carbon stars is comparable to that of FVWs, e.g., $\sim 10°$ based on the catalog of Galactic carbon stars of Alksnis et al. (2001). But the mass-loss rate of AGB stars is low ($\sim 10^{-7}\ M_{\odot}$ yr^{-1}), so the resulting 21 cm emission might be too faint.

In summary, while some of FVWs could be produced by nearby massive stars with large wind luminosity, the stellar winds or wind-blown shells from low- or high-mass protostars, or AGB stars do not seem to be capable of producing most of FVWs.

5. CONCLUSION

A "forbidden-velocity wing" (FVW) appears as a faint extended winglike feature in the large-scale (ℓ, v) diagram. Since they have excessive emission at high velocities forbidden by the Galactic rotation, there should be some dynamical phenomena associated. Thus, FVWs are closely related to the dynamical energy sources in the Galaxy and their effects on the ISM.

In this paper, we have identified 87 FVWs in the Galactic plane in use of the LDS and the SGPS data. FVWs show double-peak distribution in longitude. They have wide FWHM of about 13° in latitude and slightly skewed to positive latitude. About 70% of FVWs do have positive LSR velocities. These statistical properties appear to reflect the identifiability of FVWs in the first place, e.g., how smooth and sharp the boundary of the general Galactic H I emission is in the (ℓ, v) diagram. But there are properties that appear to be intrinsic too, e.g., the small number of FVWs at $\ell = 130°$–$180°$. The column densities of most FVWs are less than 8×10^{19} cm^{-2}. We compared the catalog of FVWs with those of SNRs, galaxies, and HVCs, and we found that $\sim 85\%$ are not coincident with those known objects.

We investigated the possibility that FVWs could be the old H I SNRs invisible in the radio continuum (KK04). The distribution of FVWs is different from that of the expected H I SNRs, and the FWHM of FVWs is wider than that of SNRs. The possibility of FVWs to be the old H I SNRs is not promising in this regard. Instead, a good fraction of FVWs may be related to anomalous velocity clouds or O-type/WR stars.

About 30% of FVWs unrelated to the known sources have discrete H I bumps that are a bit separated from the Galactic H I. Those FVWs could be isolated clouds similar to the newly discovered halo clouds (Lockman 2002). About 15% of FVWs unrelated to the known sources have nearby O-type stars. Thus, these FVWs could be due to the stellar winds from those stars. The origin of the remaining 55% of FVWs unrelated to the known sources is uncertain. In a sense that the H I SNRs are, at least, strong and fast enough to be detected as FVWs, SNRs still remain as a strong candidate of FVWs. If FVWs are indeed the oldest type of SNR, that which is essentially invisible except via its H I line emission, then only high-resolution H I observations might be able to reveal their nature.

We are very grateful to Jae-Jun Lee for his help with preparing Figure 2. We would like to thank Naomi Melissa McClure-Griffiths for providing the SGPS data. We would like to thank Jay Lockman, Myung Gyoon Lee, and Ho-Seung Hwang for their valuable discussions about other possibilities of FVWs. We also thank to the anonymous referee for his/her comments that improved the presentation of this paper. This work was supported by the Korea Science and Engineering Foundation (ABRL 3345-20031017). J.-h. K. has been supported in part by the BK 21 program.

REFERENCES

Alksnis, A., Balklavs, A., Dzervitis, U., Eglitis, I., Paupers, O., & Pundure, I. 2001, Baltic Astron., 10, 1
Bally, J., & Stark, A. A. 1983, ApJ, 266, L61
Bieging, J. H. 1990, in ASP Conf. Ser 12, Evolution of the Interstellar Medium, ed. L. Blitz (San Francisco: ASP), 137
Blitz, L., Spergel, D. N., Teuben, P. J., Hartmann, D., & Burton, W. B. 1999, ApJ, 514, 818
Boulva, F. 1999, IAPPP, 76, 84
Braun, R., & Strom, R. G. 1986, A&AS, 63, 345
Brogan, C. L., Gelfand, J. D., Gaensler, B. M., Kassim, N. E., & Lazio, T. J. W. 2006, ApJ, 639, L25
Burton, W. B., Braun, R., Walterbos, R. A. M., & Hoopes, C. G. 1999, AJ, 117, 194
Cappa, C. E., & Herbstmeier, U. 2000, AJ, 120, 1963
Cappa, C. E., Pineault, S., Arnal, E. M., & Cichowolski, S. 2002, A&A, 395, 955
de Heij, V., Braun, R., & Burton, W. B. 2002a, A&A, 391, 159
———. 2002b, A&A, 392, 417
Fürst, E., Reich, W., Reich, P., & Reif, K. 1990, A&AS, 85, 691
Garmany, C. D., Conti, P. S., & Chiosi, C. 1982, ApJ, 263, 777
Green, D. A. 2006, A Catalogue of Galactic Supernova Remnants (Cambridge: Cavendish Laboratory)
Hartmann, D., & Burton, W. B. 1997, Atlas of Galactic Neutral Hydrogen (Cambridge: Cambridge Univ. Press)
Kang, J.-h., Koo, B.-C., & Heiles, C. 2004, in ASP Conf. Ser. 317, Milky Way Surveys: The Structure and Evolution of our Galaxy, ed. (San Francisco: ASP), 38
Knapp, G. R., Jorissen, A., & Young, K. 1997, A&A, 326, 318
Koo, B.-C., & Heiles, C. 1991, ApJ, 382, 204
Koo, B.-C., & Kang, J.-h. 2004, MNRAS, 349, 983 (KK04)
Koo, B.-C., Kang, J.-h., & McClure-Griffiths, N. M. 2004, J. Korean Astron. Soc., 37, 61
Koo, B.-C., Kang, J.-h., & Salter, C. J. 2006, ApJ, 643, L49
Koo, B.-C., & Moon, D.-S. 1997, ApJ, 475, 194
Koo, B.-C., Reach, W. T., Heiles, C., Fesen, R. A., & Shull, J. M. 1990, ApJ, 364, 178
Lizano, S., Heiles, C., Rodriguez, L. F., Koo, B.-C., Shu, F. H., Hasegawa, T., Hayashi, S., & Mirabel, I. F. 1988, ApJ, 328, 763
Lockman, F. J. 2002, ApJ, 580, L47
McClure-Griffiths, N. M. 2001, Ph.D. thesis, Univ. Minnesota
Milne, D. K. 1979, Australian J. Phys., 32, 83
Paladini, R., Burigana, C., Davies, R. D., Maino, D., Bersanelli, M., Cappellini, B., Platania, P., & Smoot, G. 2003, A&A, 397, 213
Putman, M. E., et al. 2002, AJ, 123, 873
Reed, J. E., Hester, J. J., Fabian, A. C., & Winkler, P. F. 1995, ApJ, 440, 706
Reich, W., Fürst, E., Reich, P., & Reif, K. 1990, A&AS, 85, 633
Richter, P., Sembach, K. R., & Howk, J. C. 2003, A&A, 405, 1013
Russell, A. P. G., Bally, J., Padman, R., & Hills, R. E. 1992, ApJ, 387, 219
Sato, F. 1973, PASJ, 25, 135
Stanimirović, S., et al. 2006, ApJ, 653, 1210
Stil, J. M., et al. 2006, ApJ, 637, 366
Tully, R. B. 1988, Nearby Galaxies Catalog (Cambridge: Cambridge Univ. Press)
Uyaniker, B., Landecker, T. L., Gray, A. D., & Kothes, R. 2003, ApJ, 585, 785
van der Hucht, K. A. 2001, NewA Rev., 45, 135
Wakker, B. P. 1991, A&A, 250, 499
———. 2001, ApJS, 136, 463
Wakker, B. P., & van Woerden, H. 1991, A&A, 250, 509
Weaver, R., McCray, R., Castor, J., Shapiro, P., & Moore, R. 1977, ApJ, 218, 377